ULTIMATE COMPRESSIVE STRENGTH ASSESSMENT OF UNCLEANED AND CLEANED CORRODED PLATES WITH LOCKED CRACK

Krzysztof Woloszyk*
Gdansk University of Technology, Poland
Yordan Garbatov
Centre for Marine Technology and Ocean Engineering (CENTEC), Instituto Superior Técnico, Universidade de
Lisboa, Portugal

 * Corresponding author: *krzwolos@pg.edu.pl (K.Wołoszyk)*

ABSTRACT

The work presented here investigates the structural response of cleaned corroded plates, subjected to compressive load in the presence of a locked crack, where the change of mechanical properties as a result of corrosion development and the cleaning process is also accounted for. A Finite Element model for assessing the compressive strength, considering geometric and material nonlinearities, is developed, and the analysed plates are compared with the available experimental data. An experimental design plan is generated using the Design of Experiments techniques, which quantifies the influence of the governing variables and their interactions with respect to the plate's ultimate compressive strength. With a limited number of observations, the most significant effects are identified. The corrosion degradation is revealed to be the most crucial effect leading to an effective strength reduction. It was found that, in the case of a corroded plate with a locked crack subjected to a compressive load, the most severe case is when the crack is transversely oriented. The strength reduction is slightly lower than when the corrosion degradation and the presence of a crack are considered to be a simple summation of these two effects but acting separately. The outcome of the analysis is the development of several empirical formulations that allow a fast estimation of the ultimate strength of a corroded plate, subjected to compressive load in the presence of a locked crack, accounting for different cleaning.

Keywords: Cracks,Corrosion,Design of Experiments,Plate,Ultimate Strength,FEM

INTRODUCTION

Structural elements of ships and offshore structures are degraded during their service life. The main degradation effects include corrosion degradation, fatigue cracks, and denting [1], [2]. In corrosion degradation and fatigue cracking, their existence is somewhat inherent, whereas denting is rather accidental. Thus, considering these two effects during ship hull strength evaluation seems necessary, even at the beginning of the design process.

The ultimate strength of intact structures has been studied for many years, and some recent studies are presented in [3], [4]. The impact of corrosion on the load-carrying capacity of different ship structural elements was studied, both

experimentally and numerically. Experimental studies on the box girder, which simulate the real ship cross-section, were performed [5], [6]. It was found that corrosion degradation can cause a very significant reduction. In line with these findings, the analysis performed for other structural elements show similar behaviour, i.e. for stiffened panels [7], stiffened plates [1], [8], plates [9] and beams [10]. The two factors cause capacity loss. Firstly, the apparent reason is the thickness reduction. Secondly, it was discovered that the mechanical properties of steel elements with corrosion development are reduced [11]–[13].

At a micro-scale, the material properties of the steel itself are not changed by the corrosion development. However, on a large scale, such as a typical coupon specimen, the

reduction of the mechanical properties is mainly caused by the nonregularities in the corroded surfaces, which was shown in different studies for both thin [14], [15] and thick specimens [16]. These findings are in line with tensile tests of corroded and cleaned specimens [13], which show that, when specimens are subjected to different cleaning methods, the corroded surface becomes smoother and the mechanical properties are higher than corroded, non-cleaned specimens. Combining these two phenomena (i.e. subsequent thickness and mechanical properties reduction) in the Finite Element model, shows a very good agreement with the experimental results presented for stiffened plates [1]. Similar observations could be found in [17]highly ductile member, where the seismic performance of corroded H-shaped steel columns was studied. The FE model considering both thickness reduction and material properties changes, reveals very good agreement between numerical and experimental results. Thus, it is concluded that such a model could predict the strength behaviour of different structural elements subjected to corrosion degradation, despite the mechanical properties obtained via testing of small-scale coupon specimens.

Although the cracks should be detected during surveys, there will always be some level of non-detected cracks [18] for various reasons, especially in hard-to-reach places. Thus, cracks should be taken into account during the strength evaluation of the structural components. Apart from that, predicting the impact of such phenomena on structural integrity is valuable in terms of the risk assessment of ageing ships [19]. The non-propagating cracks (locked cracks) are usually taken into account in such analysis.

Similar to the corrosion degradation, the influence of locked cracks on the capacity of structural components was also investigated. However, in this case, the experimental studies are somewhat limited. The importance of this problem was first outlined in [20], [21], where the buckling stress of transversely cracked plates was evaluated. Furthermore, in [22], comprehensive elasto-plastic collapse analysis was performed, both experimentally and numerically. It was found that the strength reduction of plates can reach a level of 50%. Additionally, the FE modelling was found to be a useful tool for predicting such phenomena.

The review of the ultimate strength of cracked structural elements in ships was carried out in [23], showing examples of experimental studies with regards to plates [22], [24] and stiffened plates [25]. Much greater attention was paid to numerical studies [26]–[29]. The studies revealed the governing factors that play the most significant role in reducing the structural capacity, i.e. crack length and crack orientation. The most severe case was found to be a transverse crack in the loading direction. Some empirical formulations to assess the ultimate strength of cracked plates were derived [22], [30], [31].

However, no studies analysed the ultimate strength of plates subjected to general marine corrosion and locked cracks. Recently, some preliminary studies have examined simultaneous pitting corrosion and locked cracks [32], where it was found that these two degradation effects can occur simultaneously and may cause a very significant reduction in the plate's ultimate strength. However, it needs to be noted that pitting corrosion is a lot different from general marine corrosion.

The presented study aims to analyse the simultaneous corrosion and locked cracks, associated with the ultimate strength of plates subjected to compressive loadings. In terms of corrosion degradation, the subsequent thickness reduction and changing mechanical properties are considered. To analyse the mutual effect of the considered design variables, Design of Experiments techniques were used to make a proper experimental plan. Based on this, information about the most critical factors and their interactions were established. Finally, the simple formulations for a fast estimation of ultimate plate stress, in the presence of cracks and corrosion degradation, were obtained.

MECHANICAL PROPERTIES OF CORRODED PLATES

The experimental results presented in [12], were used to model the mechanical properties of corroded steel plates by considering different cleaning methods. The constitutive models of the mechanical properties change as a function of the degradation level, and they were developed based on the best-fit curves, as shown in Fig. 1 and 2
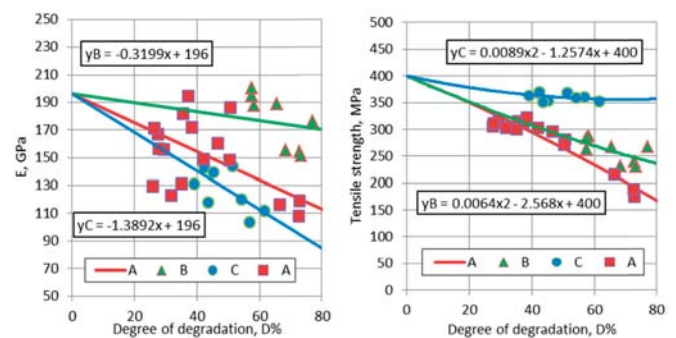

Fig. 1. Young's modulus (left) and tensile strength (right) as a function of Degree of Degradation [12] (A – corroded non-cleaned, B – corroded sandblasted, C – corroded sandpaper cleaned).
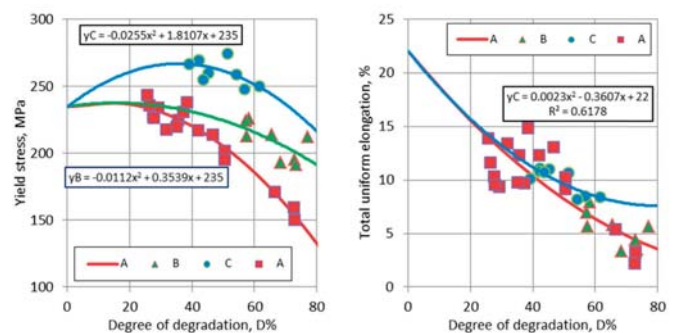

Fig. 2. Yield stress (left) and total uniform elongation (right) as a function of Degree of Degradation [12] (A – corroded non-cleaned, B – corroded sandblasted, C – corroded sandpaper cleaned).

As can be seen, all mechanical properties are reduced by corrosion development and this is measured in terms of a Degree of Degradation level (DoD), which is defined as the volumetric loss of the material, given as a percentage of the initial volume of the item. However, it needs to be noted that the yield stress is not reduced in the region between 0% and 25%. This is not in line with the findings of [15], [16], where a reduction of between 10% and 20% was observed for that region. The reason is that, in [11], the initial mechanical properties of non-corroded material was unknown and the minimum required properties for normal strength steel were considered. The minimum necessary yield stress for normal strength steel was equal to 235 MPa. To meet those criteria, during steel production, much higher yield stress values are typically observed, considering different uncertainties related to the fabrication process. The multiple tensile tests of normal strength steel, fabricated during the last couple of years and with a total number of 5,493 observations, were performed in [33]. These showed a mean value of yield strength equal to 284.5 MPa. With a significantly lower number of observations, the mean value of the yield stress was equal to 400 MPa [34].

To show real behaviour, it is assumed that the initial material properties are unknown, and they are established from extrapolation from other measured points (see Fig. 3). Based on this, the obtained value for DoD equal to 0 is taken as the initial yield stress (284.4 MPa). This is in line with the typically observed yield stress values of normal strength steel [33]. Additionally, the reduction of the yield stress for DoD equal to 25% is at the level of 15%, similar to observations made by other researchers [15], [16].
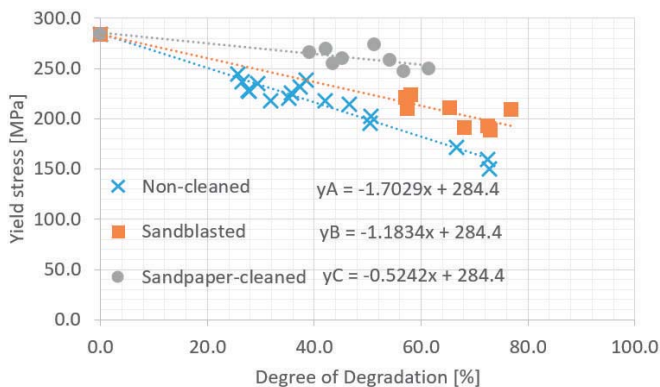

Fig. 3. Adjusted yield stress model as a function of DoD.

The initial values are similar to the typically observed values in other mechanical properties and there is no need for adjustment.

FE ANALYSIS OF ULTIMATE STRENGTH OF NON-CORRODED PLATE

To analyse the behaviour of a corroded and cracked plate subjected to compressive loads, the nonlinear Finite Element Method (FEM) was employed, considering both geometrical and material nonlinearities. The material model is considered to be bilinear with hardening. As shown in the previous section, the mechanical properties depend on the Degree of Degradation level (the percentage of mass plate reduction regarding the intact condition), considering the adjusted yield stress curve. The commercial software ANSYS [35] was used with the static implicit solver, employing the Newton-Raphson iterative procedure. SHELL181 elements were used to model the plate, and contact between the cracked edges was modelled using CONTAC52 elements. When the gap between crack edges was closed for a particular pair of nodes, the contact bonds their displacement in the longitudinal direction.

These are modelled as a half-sin wave, as suggested by Smith [36], to consider the initial plate imperfections. The average level of imperfections can be regarded as $0.1\beta t^2$, where β is the plate slenderness ratio and is equal to:

$$\beta = \frac{w}{t}\sqrt{\frac{Re}{E}} \qquad (1)$$

where w is the plate width, t is the plate thickness and Re, and E are yield stress and Young's modulus of the material, respectively. It needs to be noted that the initial thickness of the plate and the initial mechanical properties were taken into account when the initial imperfections were estimated. These originated from the welding process, and it is assumed that there are no changes in corrosion development.

The plate considered in this study is part of a ship hull, which is spanned between transverse girders in the longitudinal direction and between two stiffeners in the transverse direction. Usually, the transverse girders are very rigid, and the behaviour of loaded edges can be considered to be something between clamped or simply supported boundary conditions. In the presented study, the loaded edges were regarded as clamped. In the case of unloaded edges, the side stiffeners were not very rigid and simply supported conditions were assumed. Additionally, the longitudinal displacement of one of the loaded edges was considered to be coupled. The FE model of the corroded and cracked plate considering applied boundary conditions, is presented in Fig. 4.
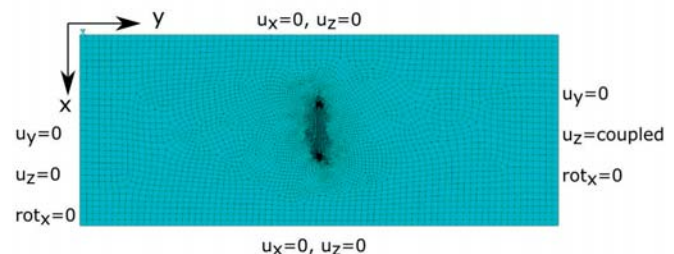

Fig. 4. FE model of the cracked and corroded plate with applied boundary conditions.

Convergence studies needed to be performed to find the optimum mesh density. The initial analysis parameters are

presented in Table 1. The FE runs for the different element sizes were performed. In terms of crack modelling, the cracked edges gap is considered equal to 2 mm and crack tips are regarded as semi-circular ones. The crack length is considered to be 1/3 of the plate width. It is known that when the crack length exceeds a certain level, it is unable to stop propagating [22].

Tab. 1. Initial parameters of the analysis.

Parameter	Symbol	Value	Unit
Plate length	l	1.5	m
Plate width	w	0.6	m
Plate thickness	t	10.5	mm
Crack length	CL	0.2	m
Crack orientation	α	0	degrees
Corrosion degradation level	DoD	12.5	%

The mesh convergence results are presented in Fig. 5. In the vertical axis, the normalised ultimate strength, which is the ultimate stress divided by the material's yield stress, is shown. At this point, and in further analysis, the initial yield stress of the non-corroded plate is considered for the calculation of the normalised ultimate capacity and initial thickness for the ultimate stress. Because of this, the corrosion influence on the load-carrying capacity, regarding the initial design conditions, is highlighted. Regarding the mesh refinement analysis, with a finite element size of 20 mm, one can get very close results to the model with the smallest element size of 5 mm. With further mesh refinement, one gets only slightly improved results with a significantly increased computational time. For these reasons, the 20 mm element size is considered in further analysis.
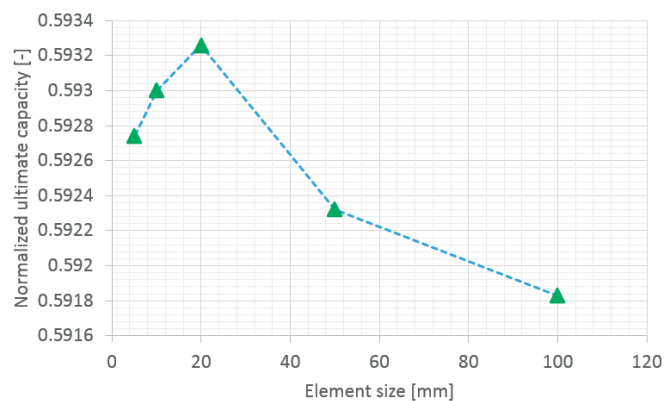

Fig. 5. Mesh refinement studies.

The welding-induced, residual stresses are not considered in the present study. However, the plate ultimate strength can be reduced in intact conditions [36]. It was shown in [37] that, when the plate is subjected to multiple loading cycles (as it is in ship structures over a couple of years of operation), the residual stresses are released. This phenomenon is known as a shakedown effect. In the case of both cracks and corrosion, their existence may be considered in ships operating for a relatively long time. Based on that information, the simultaneous existence of degradation effects and residual stresses may be neglected.

In our previous work [31], the validation of the FE model of the intact plate was performed, and showed good agreement with available experimental data and empirical formulations. In the case of degradation effects, the corrosion model was already verified in [1], where subsequent thickness reduction and changes in mechanical properties were adopted in the FE model of stiffened plates, showing good agreement with experimental results. In terms of a cracked plate, the use of FE analysis was verified by experimental results in different studies, such as [22].

EMPIRICAL ULTIMATE STRENGTH ASSESSMENT OF CORRODED PLATE

Having two effects that can influence the ultimate strength, one needs to choose the proper experimental techniques. The One Factor At a Time (OFAT) [39] analysis is performed in the classical approach. In that case, the initial design parameters are unchanged, and only one factor is varied to show its influence on the response. However, in that case, possible interaction between factors cannot be traced.

Additionally, it requires quite a significant number of observations. Experimental planning, based on the Design of Experiments (DOE) [40] techniques, seems to be more suitable to avoid that. When using this methodology, all relevant factors can be investigated in one experiment, which leads to the quantification of factor importance and the interactions between them.

Firstly, a proper design plan needs to be adopted. In this way, the Full Factorial Design (FFD) [38] was revealed to be an excellent option, especially when investigating some phenomena for the very first time. In that case, the 2^f cases were analysed, where f is the number of considered factors that influence the response. The considered factors and their symbols, together with the considered ranges of variability, are presented in Table 2.

Tab. 2. Factors considered in DoE.

Factor	Symbol	Minimum	Maximum	Unit
Plate aspect ratio (l/w)	A	1	4	-
Plate slenderness ratio (β)	B	1.524	2.857	-
Crack orientation (α)	C	0	90	degrees
Degree of Degradation (DoD)	D	0	25	%

Plate aspect ratio and slenderness ratio are general design parameters that typically influence the ultimate strength. Thus, the minimum and maximum aspect ratios were taken as 1 and 4, respectively. As presented in [42], the statistics for various types of ships were performed regarding the plate slenderness ratio. The typical value of the plate slenderness

ratio varies between 1.4 and 2.5, considering the design values of mechanical properties. In the present study, the thickness was considered from 8 mm (β = 2.857) up to 15 mm (β = 1.524). The 0° orientation crack corresponds to the transverse crack's loading direction, and the 90° crack corresponds to the longitudinal crack. In corrosion degradation, the 25% value is the level that is accepted to exist by the Classification Societies. Above that level, the plates are usually replaced. The thickness of the corroded plate was calculated based on the DoD value, assuming that it will result in a uniform loss of material. Subsequently, the changes in mechanical properties were taken into account.

In the full factorial matrix, the 2^4 = 16 number of cases was computed, and four factors considered. In this type of experiment, only the maximum or minimum values of the factors are considered. It can be seen that the linear behaviour between the extreme values is assumed. The assumption will be further validated with an additional number of cases. The upper and lower limits of the variables were considered to be equal to +1 and -1, respectively. The full factorial matrix for the FFD experiment is presented in Table 3, and the ultimate stress, as an output of FE analysis, is shown for each considered case.

Tab. 3. Full factorial test matrix with normalised ultimate stress.

Observation number	Plate aspect ratio	Plate slenderness ratio	Crack Orientation	Degree of Degradation level	Normalised ultimate stress [-]
	A	B	C	D	
1	-1	-1	-1	-1	0.739
2	-1	-1	-1	1	0.433
3	-1	-1	1	-1	0.894
4	-1	-1	1	1	0.498
5	-1	1	-1	-1	0.578
6	-1	1	-1	1	0.341
7	-1	1	1	-1	0.623
8	-1	1	1	1	0.351
9	1	-1	-1	-1	0.762
10	1	-1	-1	1	0.476
11	1	-1	1	-1	0.999
12	1	-1	1	1	0.604
13	1	1	-1	-1	0.726
14	1	1	-1	1	0.327
15	1	1	1	-1	0.725
16	1	1	1	1	0.318

The DOE provides experimental plans that are very effective and contains the statistical tools to evaluate the importance of each considered factor and the interaction between them, which are based on the Analysis of Variance (ANOVA) [39]. Furtherly, the statistical analysis regarding the results presented in Table 3 is presented.

To show the impact of each factor and their interactions, the effect values are calculated based on the average responses:

$$Eff = \frac{\sum Response_+}{n_+} - \frac{\sum Response_-}{n_-} \qquad (2)$$

where $Response_+$ is the response for the positive value of a factor or their multiplication, and $Response_-$ is the response for the negative value of a factor or their multiplication. Accordingly, n_+ is the number of cases with a positive value and n_- is the number of cases with a negative value. In this study, $n_+ = n_- = 8$.

Four main effects (A, B, C, and D) and 11 interaction effects (AB, AC, BC, AD, BD, CD, ABC, ABD, ACD, BCD, and ABCD) exist, so the total effects number is 15. The factor, or their interaction, is more important when the absolute value of the effect is higher.

To distinguish if the effect is essential or not, several techniques may be utilised. One possible technique is to sort the effects and calculate their cumulative probability values [40]. Furthermore, the half-normal probability plot is prepared, as shown in Fig. 6. The detailed procedure for the generation of such plots are found in [40]. The significant effects are those that lie on the right-hand side of the dashed line. Eventually, the effects that lie directly on the line may be influential, which needs to be judged. In principle, the line distinguishes the essential effects from those with a lower value than the statistical deviation of the results. The following factors were relevant, based on the presented half-plot: A, B, C, D, BC, AD, CD, ABD.
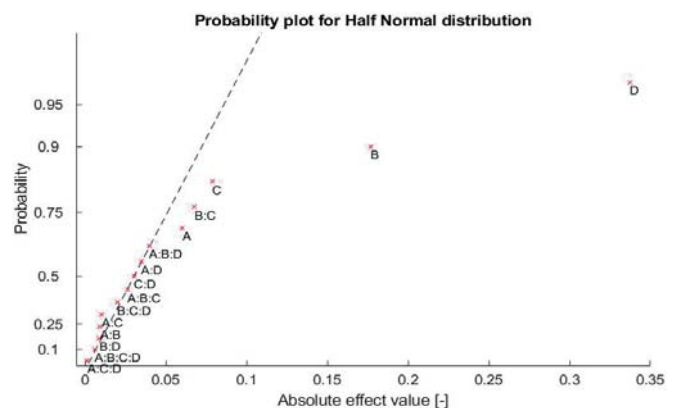

Fig. 6. Half-normal probability plot for effects.

Another possible way to distinguish the significant and insignificant effects, is to perform the t-test for each considered effect. An example of this type of analysis may be found in [31]. Usually, both methodologies lead to the same conclusions. The significant effects, ranked from most important to least important, are presented in Table 4.

Tab. 4. Effect ranking.

Rank	Effects	Absolute value of effect [-]
1	D (degree of degradation)	0.3371
2	B (plate slenderness ratio)	0.1767
3	C (crack orientation)	0.0786
4	BC	0.0676
5	A (plate aspect ratio)	0.0601

Rank	Effects	Absolute value of effect [-]
6	ABD	0.0395
7	AD	0.0346
8	CD	0.0302

The study shows very interesting results that need to be discussed. The most important factor is the degree of degradation, which reveals that corrosion degradation is the most dangerous ageing phenomenon. The results show that the plate with the considered level of corrosion degradation of 25% may have a reduced capacity of up to 56%, and the mean level of capacity reduction is equal to 45%.

The next most-influential parameter is the plate slenderness ratio, and it is known that the ultimate strength is reduced at higher values of this parameter. This is explained by the fact that more slender plates have a lower value of theoretical buckling stress, and so they are more prone to premature failure than stockier plates.

The third most important factor is crack orientation. When the crack orientation is longitudinal, no significant reduction of the capacity is observed [31]. The most dangerous are the transverse cracks. Based on the results, the most important difference between the ultimate stress for the longitudinal and transverse crack position reaches 23%, and the mean level of the capacity reduction is about 10%.

The least influential main effect is the plate aspect ratio. In general, the ultimate strength is higher for higher values. Furthermore, it was found that the failure mode will differ, mainly depending on the plate slenderness ratio. For a high slenderness ratio, the ultimate strength will be caused primarily by elastic buckling and, usually, several half-sin waves of loss of stability in the post-collapse form will be observed. In this case, ultimate strength will be lower. For a low slenderness ratio, the ultimate strength will be dominated by the plastic collapse and only one half-sin wave in post-collapse form is observed. For this case, higher values of ultimate strength will be observed. No significant influence of the corrosion degradation level was found on the failure mode.

The most interesting part of the results is related to the revealed interaction effects. The most significant interaction effect is the interaction between the plate slenderness ratio and crack orientation. When the slenderness ratio is low, the influence of the crack orientation on the ultimate strength is very high. However, the ultimate strength is not so severely reduced with different orientation angles for the slender plates. It may be concluded that crack existence is much more dangerous for stocky plates. Another significant interaction effect is the interaction between three factors: the plate aspect ratio, plate slenderness ratio and degree of degradation. Due to the involvement of the three factors, the interpretation is not straightforward. However, based on the analysis of the results, the ultimate strength is higher when plate slenderness ratio and aspect ratio have different signs for a high level of corrosion degradation. For example, for a low aspect ratio and slenderness ratio, the ultimate strength is lower than the plate with a low aspect ratio and a high slenderness ratio.

Furthermore, the interaction between the plate aspect ratio and corrosion degradation level was found. The ultimate strength is more reduced when corrosion exists for plates with a high aspect ratio than the plates with a low aspect ratio. Finally, the interaction effect between the crack orientation and corrosion degradation was found. From analysis of the results, it can be seen that, when there is a simultaneously high degradation level and transverse crack orientation, the ultimate strength is slightly higher than a simple superposition of these two degradation effects. In first case, the reduction of ultimate strength is equal to 51% and it is less than the sum of the mean reductions of the capacity caused by the crack (10%) and corrosion degradation (45%). Nevertheless, it is noted that the plate capacity is most severely reduced when considering these two effects simultaneously.

A simple regression model (Response Surface) can be obtained based on the results. This formula is beneficial at the design stage, to avoid complicated analysis and allow for the first estimation of considered strength. In the case of FFD, the Response Surface takes the form of a linear regression model. When considering the main effects and interaction of two or three effects, the model will take the general form:

$$\bar{y} = B_0 + \sum_{i=1}^{f} B_i x_i + \sum_{i<j=2}^{f}\sum B_{ij} x_i x_j + \sum_{i<j<k=3}^{f}\sum B_{ijk} x_i x_j x_k \quad \text{(3)}$$

where x_i are the model variables and the parameters B_i, B_{ij}, B_{ijk} are the linear coefficients. There are equal to half of the previously obtained effect values. However, one needs to be aware that the absolute values of effects were considered in importance analysis. In linear coefficients, they can be positive or negative, depending on their influence on the response value. The value of B_0 is taken as a mean value from all analysed cases.

To normalise the variables, which were taken in the range between -1 and 1 in DoE analysis and are different from the real variable ranges shown in Table 2, the following values were calculated:

$$x_1 = \frac{\left(\frac{l}{w}\right) - 2.5}{1.5} \quad \text{(4)}$$

$$x_2 = \frac{\beta - 2.19}{0.666} \quad \text{(5)}$$

$$x_3 = \frac{\alpha - 45}{45} \quad \text{(6)}$$

$$x_4 = \frac{DoD - 12.5}{12.5} \quad \text{(7)}$$

The parameters of the response surface are $B_0 = 0.5871$, $B_1 = 0.03007$, $B_2 = -0.08836$, $B_3 = 0.03928$, $B_4 = -0.1686$, $B_{23} = -0.03379$, $B_{14} = -0.01732$, $B_{34} = -0.01511$, $B_{124} = -0.01977$.

The final response surface takes the form:

$$\overline{y_1} = 0.5871 + 0.03007\,x_1 - 0.08836\,x_2 + 0.03928\,x_3 - 0.1686\,x_4 + \\ - 0.03379\,x_2 x_3 - 0.01732\,x_1 x_4 - 0.01511\,x_3 x_4 - 0.01977\,x_1 x_2 x_4 \quad \textbf{(8)}$$

Eq. (8) gives a fast estimation of the ultimate strength when corrosion and cracking in the compressively loaded plate are considered. However, the following model only considers a linear relationship between the factors and response. This may be different when compared with the exact FE solutions. To get a better estimation level, the Central Composite Design (CCD) can be considered. In this experimental plan, extreme values of the variables were considered at a central point (all variables equal to 0) and axial points (only one variable is equal to 1 or -1, where others are equal to 0). This allows for the derivation of a quadratic response surface. In this case, the total number of considered cases is equal to $2^f + 2f + 1$, so it is equal to 25 in the analysed problem.

To see whether the more advanced formulation is needed or not, additional FE runs for axial and central points were performed, and the results compared to the estimation using Eq. (8). The results for additional points, together with the factorial matrix, are presented in Table 5.

Tab. 5. Factorial matrix for additional design points.

Observation number	Plate aspect ratio	Plate slenderness ratio	Crack Orientation	Degree of degradation	Normalised ultimate stress [-]	
	A	B	C	D	FEM	Eq. (8)
17	0	0	0	0	0.628	0.587
18	-1	0	0	0	0.536	0.557
19	1	0	0	0	0.628	0.617
20	0	-1	0	0	0.654	0.675
21	0	1	0	0	0.528	0.499
22	0	0	-1	0	0.593	0.548
23	0	1230	1	0	0.689	0.626
24	0	0	0	-1	0.781	0.756
25	0	0	0123123	1	0.454	0.419

The comparison of the exact FE results and estimated values from Eq. (8) is presented in Fig. 7. In the case of FFD points, the regression line is plotted, showing excellent performance with the R^2 value of 0.992. In this case, the mean error of the estimation is 2.4%. In the case of additional CCD points, it can be seen that the points lie below the curve. This means that, in general, the formula underestimates the value of the ultimate strength for those points. The mean error of the estimation is 5.4%. This lead to the conclusion that the derivation of a quadratic response surface may reduce the uncertainty level for those points.
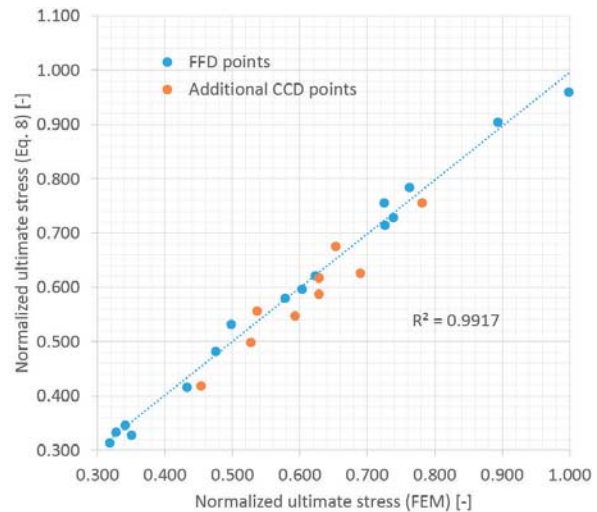
Fig. 7. Comparison between response surface estimation and exact solution.

In this case, when values from the CCD plan are considered, the response surface takes a general form of:

$$\bar{y} = B_0 + \sum_{i=1}^{f} B_i x_i + \sum_{i=1}^{f} B_{ii} x_i^2 + \sum_{i<j=2}^{f} B_{ij} x_i x_j + \sum_{i<j<k=3}^{f} B_{ijk} x_i x_j x_k \quad \textbf{(9)}$$

By analysing the results, it was found that three of the four variables influence the response in a nonlinear way: plate slenderness ratio, plate aspect ratio and crack orientation. The new response surface, based on the CCD experimental results, was established with three new coefficients and changed B_0 value:

$$\overline{y_2} = 0.6173 + 0.03007\,x_1 - 0.03348 x_1^2 - 0.08836\,x_2 - 0.02448 x_2^2 + 0.03928\,x_3 + \\ +0.02552 x_3^2 - 0.1686\,x_4 - 0.03379\,x_2 x_3 - 0.01732\,x_1 x_4 - 0.01511\,x_3 x_4 - 0.01977\,x_1 x_2 x_4 \quad \textbf{(10)}$$

To compare the improved formulation from Eq. (10), the estimated ultimate strength results are again compared with the exact FE solutions, as presented in Fig. 8.
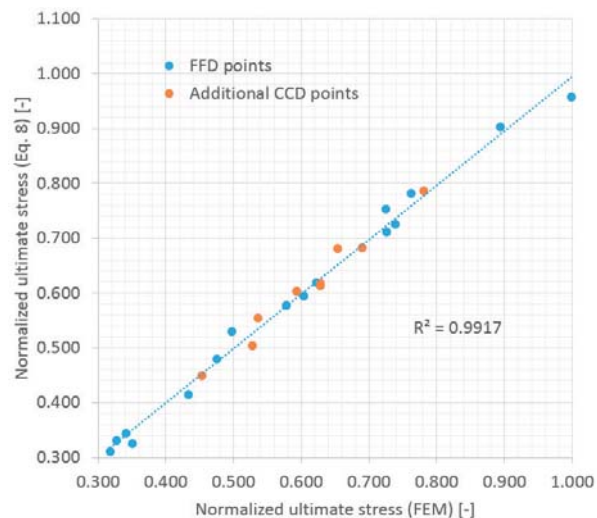
Fig. 8. Comparison between improved response surface estimation and exact solution.

One can see that, in the FFD points, the plot is similar to that in Fig. 7. However, the estimated results for additional CCD points are much closer to those obtained from the FE computations. In this case, the mean error of the estimation for all cases is about 2.4%.

As can be seen, the two simple formulations were derived based on 16 cases for a linear approximation and 25 cases for a quadratic approximation. Nevertheless, with the limited number of FE analysis runs, the impact of the governing factors, together with their interactions, was obtained. This number of cases seems to be reasonable even when performing physical tests.

EMPIRICAL ULTIMATE STRENGTH ASSESSMENT OF CLEANED CORRODED PLATES METHODS

Similar to the methodology presented in the previous section, two design curves were developed, considering the corroded plates cleaned by sandblasting and sandpaper cleaning techniques. The mechanical properties were deemed to be present in the second section, and design variables were taken to be as shown before. In both cases, the CCD experimental plan was applied, leading to quadratic response surfaces; similar effects were revealed to be the most important ones. As a result, two solutions were established. The normalised ultimate strength, considering the sandblasted surface of the corroded plate, is defined as:

$$\overline{y_3} = 0.6343 + 0.0331\,x_1 - 0.03673x_1^2 - 0.08617\,x_2 - 0.0212x_2^2 + 0.0424\,x_3 + \\ +0.0273x_3^2 - 0.1537\,x_4 - 0.0346\,x_2x_3 - 0.0155\,x_1x_4 - 0.0135\,x_3x_4 - 0.0191\,x_1x_2x_4 \quad \textbf{(11)}$$

The normalised ultimate strength, considering the sandpaper-cleaned surface of the corroded plate, is defined by:

$$\overline{y_4} = 0.6276 + 0.0278\,x_1 - 0.019\,x_1^2 - 0.0952\,x_2 - 0.0215\,x_2^2 + 0.0381\,x_3 + \\ +0.028\,x_3^2 - 0.1571\,x_4 - 0.0331\,x_2x_3 - 0.0217\,x_1x_4 - 0.0174\,x_3x_4 - 0.0258\,x_1x_2x_4 \quad \textbf{(12)}$$

To analyse the impact of mechanical property changes, considering different types of surface cleaning, a reference model considering only the thickness reduction due to corrosion development, without considering the difference in the mechanical properties, is provided as:

$$\overline{y_5} = 0.6692 + 0.0328\,x_1 - 0.03688\,x_1^2 - 0.09278\,x_2 - 0.02738\,x_2^2 + 0.0421\,x_3 + \\ +0.0246\,x_3^2 - 0.132\,x_4 - 0.03575\,x_2x_3 - 0.0168\,x_1x_4 - 0.01338\,x_3x_4 - 0.02263\,x_1x_2x_4 \quad \textbf{(13)}$$

It can be seen that the plate slenderness ratio and degree of corrosion degradation are primary factors that govern the ultimate compressive strength. To analyse the differences between the studied solutions, the plate aspect ratio is considered to be 1, and only one transverse crack is assumed. Furthermore, plots comparing the reference model, which does not account for the mechanical property changes, are compared to those that account for mechanical property change, due to the corroded plate surface cleaning presented in Fig. 9.

There are significant differences between the case when only the thickness reduction of the corroded plate is considered in the ultimate strength assessment, compared to the mutual effect of the thickness reduction and mechanical property changes, as a result of corrosion degradation. In general, the ultimate strength drops with the increase of both degrees of degradation and plate slenderness ratio, for all cases. In terms of cleaning methods, sandblasting only results in a slightly higher ultimate strength than the uncleaned corroded plate. However, the resulting ultimate strength is closer to the case where the mechanical property change is not considered in sandpaper cleaning. The ultimate strength of non-cleaned corroded surfaces is lower compared to cleaned ones. This is caused by the lower reduction of mechanical properties in cleaned plates and smoothing of the level of sharpness of the pits by cleaning (see Fig. 3).

The presented formulations can be adopted for assessing the compressive strength of corroded, cleaned plates as a function of the degree of degradation and cleaning approach. Additionally, based on the developed formulation for corroded cleaned plates, one can define the most appropriate cleaning method, from the point of view of compressive strength.
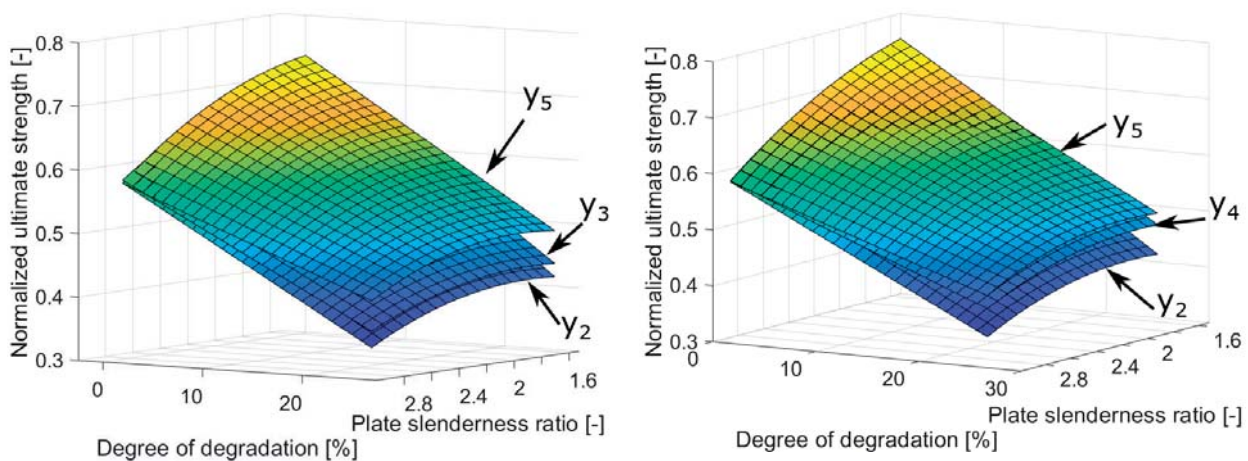

Fig. 9. Normalised ultimate strength: (non-cleaned corroded surface), (corroded and sandblast-cleaned surface), (corroded and sandpaper-cleaned surface); (non-cleaned corroded surface, without considering the change in mechanical properties).

CONCLUSIONS

The objective of this study was to analyse the mutual effects of corrosion degradation and the presence of a locked crack, where the change of mechanical properties (as a result of corrosion development) is also accounted for, leading to a significant decrease in the ultimate strength of a plate subjected to compressive load. Besides the degradation effects, the plate slenderness ratio and plate aspect ratio were considered to be design variables. An experimental design plan was performed with the use of DoE techniques, considering both Full Factorial Design, as well as Central Composite Design. The workflow of computations showed that, with a properly designed experiment, one can obtain information about the impact of each governing factor and their interactions in a straightforward way. Nevertheless, the computational effort is somewhat limited concerning the information obtained.

Regarding the ultimate compressive strength, the degree of corrosion degradation was the most critical factor. The second influential factor was the plate slenderness ratio, followed by locked crack orientation and plate aspect ratio. Additionally, four interaction effects were found to be important. The corrosion degradation, as a separate effect, lead to approximately 45% strength reduction, whereas transversely oriented cracks lead to 10% ultimate strength reduction. When significant corrosion degradation and locked cracks are acting simultaneously, the compressive strength reduction is about 51%, which is less than the simple sum of their impact. Nevertheless, the existence of these two factors at one time is the most critical case.

Two empirical formulations were developed for the fast estimation of the ultimate strength of a plate, subjected to compressive load in the presence of a locked crack and corrosion degradation. The second formulation is based on the quadratic approach and showed an excellent performance in the entire design space. Nevertheless, further studies relating to the applicability of the developed formulations still need to be carried out before they can be used directly in practical applications.

In addition, the developed empirical formulations for the ultimate compressive strength, considering different types of corroded plate surface cleaning approaches, are compared with a reference model, where no mechanical property changes were considered. It was concluded that sandpaper cleaning is a more effective method, in terms of ultimate compressive strength resilience. The developed formulation for corroded and cleaned plates can define the most appropriate approach for cleaning from a compressive strength point of view.

REFERENCES

1. K. Woloszyk, M. Kahsin, and Y. Garbatov, "Numerical assessment of ultimate strength of severe corroded stiffened plates," *Eng. Struct.*, vol. 168, pp. 346–354, Aug. 2018, doi: 10.1016/j.engstruct.2018.04.085.

2. S. Saad-Eldeen, Y. Garbatov, and C. Guedes Soares, "Ultimate strength analysis of highly damaged plates," *Mar. Struct.*, vol. 45, pp. 63–85, Jan. 2016, doi: 10.1016/j.marstruc.2015.10.006.

3. K. Woloszyk, Y. Garbatov, J. Kowalski, and L. Samson, "Experimental and numerical investigations of ultimate strength of imperfect stiffened plates of different slenderness," *Polish Marit. Res.*, vol. 27, no. 4, pp. 120–129, 2020.

4. H. Ölmez and E. Bayraktarkatal, "Maximum Load Carrying Capacity Estimation of The Ship and Offshore Structures by Progressive Collapse Approach," *Polish Marit. Res.*, vol. 23, no. 3, pp. 28–38, Sep. 2016, doi: 10.1515/pomr-2016-0029.

5. S. Saad-Eldeen, Y. Garbatov, and C. Guedes Soares, "Ultimate strength assessment of corroded box girders," *Ocean Eng.*, vol. 58, pp. 35–47, Jan. 2013, doi: 10.1016/j.oceaneng.2012.09.019.

6. S. Saad-Eldeen, Y. Garbatov, and C. Guedes Soares, "Effect of corrosion degradation on ultimate strength of steel box girders," *Corros. Eng. Sci. Technol.*, vol. 47, no. 4, pp. 272–283, Jun. 2012, doi: 10.1179/1743278212Y.0000000005.

7. X. H. Shi, J. Zhang, and C. Guedes Soares, "Numerical assessment of experiments on the ultimate strength of stiffened panels with pitting corrosion under compression," *Thin-Walled Struct.*, vol. 133, pp. 52–70, Dec. 2018, doi: 10.1016/j.tws.2018.09.029.

8. Y. Garbatov, M. Tekgoz, and C. Guedes Soares, "Experimental and numerical strength assessment of stiffened plates subjected to severe non-uniform corrosion degradation and compressive load," *Ships Offshore Struct.*, vol. 12, no. 4, pp. 461–473, May 2017, doi: 10.1080/17445302.2016.1173807.

9. J. E. Silva, Y. Garbatov, and C. Guedes Soares, "Ultimate strength assessment of rectangular steel plates subjected to a random localised corrosion degradation," *Eng. Struct.*, vol. 52, pp. 295–305, Jul. 2013, doi: 10.1016/j.engstruct.2013.02.013.

10. Y. Wang, S. Xu, and A. Li, "Flexural performance evaluation of corroded steel beams based on 3D corrosion morphology," *Struct. Infrastruct. Eng.*, pp. 1–16, Jan. 2020, doi: 10.1080/15732479.2020.1713169.

11. Y. Garbatov, C. Guedes Soares, J. Parunov, and J. Kodvanj, "Tensile strength assessment of corroded small scale specimens," *Corros. Sci.*, vol. 85, pp. 296–303, Aug. 2014, doi: 10.1016/j.corsci.2014.04.031.

12. Y. Garbatov, J. Parunov, J. Kodvanj, S. Saad-Eldeen, and C. Guedes Soares, "Experimental assessment of tensile strength of corroded steel specimens subjected to sandblast and sandpaper cleaning," *Mar. Struct.*, vol. 49, pp. 18–30, Sep. 2016, doi: 10.1016/J.MARSTRUC.2016.05.009.

13. Y. Garbatov, S. Saad-Eldeen, C. Guedes Soares, J. Parunov, and J. Kodvanj, "Tensile test analysis of corroded cleaned aged steel specimens," *Corros. Eng. Sci. Technol.*, pp. 1–9, Nov. 2018, doi: 10.1080/1478422X.2018.1548098.

14. K. Woloszyk and Y. Garbatov, "Random field modelling of mechanical behaviour of corroded thin steel plate specimens," *Eng. Struct.*, vol. 212, p. 110544, Jun. 2020, doi: 10.1016/j.engstruct.2020.110544.

15. B. Nie, S. Xu, J. Yu, and H. Zhang, "Experimental investigation of mechanical properties of corroded cold-formed steels," *J. Constr. Steel Res.*, vol. 162, p. 105706, Nov. 2019, doi: 10.1016/j.jcsr.2019.105706.

16. Y. Wang, S. Xu, H. Wang, and A. Li, "Predicting the residual strength and deformability of corroded steel plate based on the corrosion morphology," *Constr. Build. Mater.*, vol. 152, pp. 777–793, Oct. 2017, doi: 10.1016/j.conbuildmat.2017.07.035.

17. S. Xu, Z. Zhang, and G. Qin, "Study on the seismic performance of corroded H-shaped steel columns," *Eng. Struct.*, vol. 191, pp. 39–61, Jul. 2019, doi: 10.1016/j.engstruct.2019.04.037.

18. T. Moan, O. T. Va˚rdal, N.-C. Hellevig, and K. Skjoldli, "Initial Crack Depth and POD Values Inferred From In-Service Observations of Cracks in North Sea Jackets," *J. Offshore Mech. Arct. Eng.*, vol. 122, no. 3, pp. 157–162, Aug. 2000, doi: 10.1115/1.1286676.

19. J. K. Paik, G. Wang, A. K. Thayamballi, J. M. Lee, Y. Il Park, and J. Parunov, "Time-dependent risk assessment of aging ships accounting for general / pit corrosion, fatigue cracking and local denting damage," *Trans. - Soc. Nav. Archit. Mar. Eng.*, vol. 111, pp. 159–98, 2003.

20. Y. A. Roy, B. P. Shastry, and G. V. Rao, "Stability of square plates with through transverse cracks," *Comput. Struct.*, vol. 36, no. 2, pp. 387–388, 1990, doi: 10.1016/0045-7949(90)90137-Q.

21. D. Shaw and Y. H. Huang, "Buckling behavior of a central cracked thin plate under tension," *Eng. Fract. Mech.*, vol. 35, no. 6, pp. 1019–1027, Jan. 1990, doi: 10.1016/0013-7944(90)90129-5.

22. J. K. Paik, Y. V. Satish Kumar, and J. M. Lee, "Ultimate strength of cracked plate elements under axial compression or tension," *Thin-Walled Struct.*, vol. 43, no. 2, pp. 237–272, Feb. 2005, doi: 10.1016/j.tws.2004.07.010.

23. A. Babazadeh and M. R. Khedmati, "Ultimate strength of cracked ship structural elements and systems: A review," *Eng. Fail. Anal.*, vol. 89, pp. 242–257, Jul. 2018, doi: 10.1016/j.engfailanal.2018.03.003.

24. R. Seifi and N. Khoda-yari, "Experimental and numerical studies on buckling of cracked thin-plates under full and partial compression edge loading," *Thin-Walled Struct.*, vol. 49, no. 12, pp. 1504–1516, Dec. 2011, doi: 10.1016/j.tws.2011.07.010.

25. X. H. Shi, J. Zhang, and C. Guedes Soares, "Experimental study on collapse of cracked stiffened plate with initial imperfections under compression," *Thin-Walled Struct.*, vol. 114, pp. 39–51, May 2017, doi: 10.1016/j.tws.2016.12.028.

26. A. Rahbar-Ranji and A. Zarookian, "Ultimate strength of stiffened plates with a transverse crack under uniaxial compression," *Ships Offshore Struct.*, vol. 10, no. 4, pp. 416–425, Jul. 2015, doi: 10.1080/17445302.2014.942078.

27. C. Cui, P. Yang, C. Li, and T. Xia, "Ultimate strength characteristics of cracked stiffened plates subjected to uniaxial compression," *Thin-Walled Struct.*, vol. 113, pp. 27–38, Apr. 2017, doi: 10.1016/j.tws.2017.01.003.

28. S. Saad-Eldeen, Y. Garbatov, and C. Soares, "Emergency repair of a single hull structure with locked cracks," in *Maritime Technology and Engineering III*, CRC Press, 2016, pp. 521–529.

29. S. Saad-Eldeen, Y. Garbatov, and C. G. Soares, "Strength enhancement of cracked swash bulkheads of jack-up spud-can," in *Progress in the Analysis and Design of Marine Structures*, CRC Press, 2017, pp. 763–770.

30. A. Babazadeh and M. R. Khedmati, "Empirical formulations for estimation of ultimate strength of cracked continuous unstiffened plates used in ship structure under in-plane longitudinal compression," *Eng. Fail. Anal.*, vol. 100, pp. 470–484, Jun. 2019, doi: 10.1016/j.engfailanal.2019.02.051.

31. K. Woloszyk and Y. Garbatov, "Analysis of Ultimate Compressive Strength of Cracked Plates with the Use of DoE Techniques," *Polish Marit. Res.*, vol. 27, no. 3, pp. 109–120, Sep. 2020, doi: 10.2478/pomr-2020-0052.

32. L. Feng, D. Li, H. Shi, Q. Zhang, and S. Wang, "A study on the ultimate strength of ship plate with coupled corrosion

and crack damage," *Ocean Eng.*, vol. 200, p. 106950, Mar. 2020, doi: 10.1016/j.oceaneng.2020.106950.

33. J. Melcher, Z. Kala, M. Holický, M. Fajkus, and L. Rozlívka, "Design characteristics of structural steels based on statistical analysis of metallurgical products," *J. Constr. Steel Res.*, vol. 60, no. 3–5, pp. 795–808, Mar. 2004, doi: 10.1016/S0143-974X(03)00144-5.

34. A. J. Sadowski, J. M. Rotter, T. Reinke, and T. Ummenhofer, "Statistical analysis of the material properties of selected structural carbon steels," *Struct. Saf.*, vol. 53, pp. 26–35, Mar. 2015, doi: 10.1016/j.strusafe.2014.12.002.

35. ANSYS, "Online Manuals, Release 19." 2019.

36. M. Tekgoz, Y. Garbatov, and C. Guedes Soares, "Finite element modelling of the ultimate strength of stiffened plates with residual stresses," in *Analysis and Design of Marine Structures*, CRC Press, 2013, pp. 309–317.

37. M. Tekgoz and Y. Garbatov, "Ultimate strength of a plate accounting for shakedown effect and corrosion degradation," in *Developments in Maritime Transportation and Exploitation of Sea Resources*, CRC Press, 2013, pp. 395–403.

38. D. C. Montgomery, *Design and Analysis of Experiments*. John Wiley & Sons Ltd, USA, 2006.

39. S. M. Dowdy, S. Wearden, and D. M. Chilko, *Statistics for research*. Wiley-Interscience, 2004.

40. C. Daniel, "Use of Half-Normal Plots in Interpreting Factorial Two-Level Experiments," *Technometrics*, vol. 1, no. 4, pp. 311–341, Nov. 1959, doi: 10.1080/00401706.1959.10489866.

CONTACT WITH THE AUTHORS

Krzysztof Woloszyk

e-mail: *krzwolos@pg.edu.pl*
Gdansk University of Technology,
Narutowicza 11/12, 80-233 Gdańsk,
Poland

Yordan Garbatov

e-mail: *yordan.garbatov@tecnico.ulisboa.pt*
Centre for Marine Technology and Ocean Engineering (CENTEC),
Instituto Superior Técnico, Universidade de Lisboa,
Avenida Rovisco Pais, 1049-001 Lisboa,
Portugal